

Effects of the vortices and impurities on the nuclear spin relaxation rate in iron-based superconductors

Hong-Min Jiang,^{1,2} Jia Guo,² and Jian-Xin Li²

¹*Department of Physics, Hangzhou Normal University, Hangzhou 310036, China*

²*National Laboratory of Solid State of Microstructure and Department of Physics, Nanjing University, Nanjing 210093, China*

(Dated: February 18, 2022)

The effects of magnetic vortices and nonmagnetic impurities on the low energy quasiparticle excitations and the spin-lattice relaxation rate are examined in the iron-based superconductors for the s_{\pm} -, s - and d -wave pairing symmetries, respectively. The main effect of the vortices is to enhance the quasiparticle excitations and the spin-lattice relaxation rate for all symmetries, and leads to a T^3 dependence of the relaxation rate followed by a nearly T -linearity at lower temperatures. This enhancement can only be seen for the s_{\pm} - and d -wave symmetries in the presence of nonmagnetic impurities. These results suggest that the s_{\pm} -wave and d -wave pairing states behave similarly in response to the magnetic field and nonmagnetic impurities, therefore it may be impossible to distinguish them on the basis of the measurements of spin-lattice relaxation rates when a magnetic field and/or impurity scatterings are present.

PACS numbers: 74.20.Mn, 74.25.Ha, 74.62.En, 74.25.nj

I. INTRODUCTION

Recently much attention has been paid to the newly discovered iron arsenide superconductors,¹⁻⁵ which display superconducting transition temperature as high as more than 50K, appear to share a number of general features with high- T_c cuprates, including the layered structure and proximity to a magnetically ordered state.^{1,6,7} These observations suggest that the conventional phonon-mediated pairing mechanism appears to be unlikely and the magnetic correlations may be relevant for superconductivity. So far, unconventional superconductivity with pairing symmetry s_{\pm} mediated by the interband spin fluctuations has been proposed by a number of theories for this layered iron superconductors.⁸⁻¹¹ Although, such a popular proposal can explain some experimental findings, the situation is complicated by the power-law temperature dependence of the spin-lattice relaxation rate $T_1^{-1} \sim T^n$ below T_c with the doping dependent n varying from 6 to 1.5.¹²⁻²² Because a simple theoretical analysis shows that the relaxation rate T_1^{-1} should exhibit an exponential temperature dependence for a fully gaped superconductors, while power law relation $T_1^{-1} \sim T^3$ holds in the presence of line nodes in the SC gap. Moreover, several experiments have reported the evidence of a residual density-of-state (DOS) at zero energy in the SC state, where the temperature dependent relaxation rate deviates from the $T_1^{-1} \sim T^3$ relation and exhibits $T_1^{-1} \sim T$ behavior at very low temperature.^{13,14,23} The disparity between the theoretical proposal and the experimental fact presents a puzzle that should be resolved for the determination of the SC pairing symmetry in these high- T_c superconductors.

The relaxation rate has been studied in the presence of the impurity-enhanced quasiparticle scattering at zero field in the band representation, and it shows the power law temperature dependence $T_1^{-1} \sim T^3$ for

the $s_{\pm} = \Delta_0 \cos(k_x) \cos(k_y)$ -wave SC pairing.²⁴⁻²⁶ Although the enhancement of the quasiparticle scattering has been well included in the previous studies, the relationship between the SC gap and the impurities addressed in the band representation were debated controversially.^{27,28} More importantly, actual spin-lattice relaxation rate measured in NMR experiments are conducted under a magnetic field of several Tesla, where the relaxation rate shows the temperature dependence $T_1^{-1} \sim T^3$ and even $T_1^{-1} \sim T$.^{13,21,23,29} At the same time, H. J. Grafe *et al.* has found that the superconducting vortices contribute to the spin-lattice relaxation rate when the magnetic field is perpendicular to the conducting plane but not for the parallel direction.^{12,30} In fact, it is unclear up to now whether the different value of n in the temperature dependence of T_1^{-1} is caused by a change of the pairing symmetry with doping, a disorder scattering effect in an s_{\pm} gap superconductor, or other unknown mechanism. In view of these theoretical and experimental facts, it is necessary to compare and contrast different pairing symmetries by studying the effects of impurities and magnetic field on the spin-lattice relaxation rate in the analysis of the standardized procedure extracting the gap symmetry.

The purpose of this study is to present such a contrastive study on three different superconducting (SC) pairing symmetries with s_{\pm} -, s - and d -wave, respectively. For this purpose, we calculate the DOS and the spin-lattice relaxation rate in the Fe-based superconductors in the presence of magnetic field and nonmagnetic impurities by self-consistently solving the Bogoliubov-de Gennes equations based on the simple two-orbital model. It is shown that the characteristic low energy quasiparticle excitations depend on the gap functions in the presence of magnetic vortices and nonmagnetic impurities. The magnetic vortices contribute significantly to the spin-lattice relaxation rate and lead to the relation $T_1^{-1} \sim T^3$ followed by a nearly linear dependence at lower

temperatures for all symmetries. While in the presence of nonmagnetic impurities, this enhancement of T_1^{-1} can only be seen for the s_{\pm} - and d -wave symmetries. Thus, in the presence of magnetic field and nonmagnetic impurities, the s_{\pm} -wave pairing behaves much like what the d -wave does.

The remainder of the paper is organized as follows. In Sec. II, we introduce the model Hamiltonian and carry out analytical calculations. In Sec. III, we present numerical calculations and discuss the results. In Sec. IV, we make a conclusion.

II. THEORY AND METHOD

We start with an effective two-orbital model that takes only the iron d_{xz} and d_{yz} orbitals into account.³¹ By assuming an effective attraction that causes the superconducting pairing and including the possible interactions between the two orbitals' electrons, one can construct an effective model to study the vortex and impurity physics of the iron-based superconductors in the superconducting state:

$$H = H_0 + H_{pair}. \quad (1)$$

The first term is a tight-binding model

$$H_0 = - \sum_{ij,\alpha\beta,\sigma} e^{i\varphi_{ij}} t_{ij,\alpha\beta} c_{i,\alpha,\sigma}^\dagger c_{j,\beta,\sigma} - \mu \sum_{i,\alpha,\sigma} c_{i,\alpha,\sigma}^\dagger c_{i,\alpha,\sigma} + \sum_{i,\alpha,\sigma} U_i c_{i,\alpha,\sigma}^\dagger c_{i,\alpha,\sigma}, \quad (2)$$

which describes the electron effective hoppings between sites i and j of the Fe ions on the square lattice, including the intra- ($t_{ij,\alpha\alpha}$) and inter-orbital ($t_{ij,\alpha\beta}$, $\alpha \neq \beta$) hoppings with the subscripts α , β ($\alpha, \beta = 1, 2$ for xz and yz orbital, respectively) denoting the orbitals and σ the spin. $c_{i,\alpha\sigma}^\dagger$ creates an α orbital electron with spin σ at the site i ($i \equiv (i_x, i_y)$), and μ is the chemical potential. The magnetic field is introduced through the Peierls phase factor $e^{i\varphi_{ij}}$ with $\varphi_{ij} = \frac{\pi}{\Phi_0} \int_{r_j}^{r_i} \mathbf{A}(\mathbf{r}) \cdot d\mathbf{r}$ in the vortex state, where $A = (-Hy, 0, 0)$ stands for the vector potential in the Landau gauge and $\Phi_0 = hc/2e$ is the superconducting flux quantum. In the case of the SC state with impurities, we randomly select the half number of total sites, at where the random disorder potentials U_i uniformly distributed over $[-U, U]$ are set in. Then U is a parameter to characterize the strength of the disorder. The hopping integrals are chosen as to capture the essence of the density function theory (DFT) results.³² Taking the hopping integral between the d_{yz}

orbitals $|t_1| = 1$ as the energy unit, we have,

$$\begin{aligned} t_{i,i\pm\hat{x},xz,xz} &= t_{i,i\pm\hat{y},yz,yz} = t_1 = -1.0 \\ t_{i,i\pm\hat{y},xz,xz} &= t_{i,i\pm\hat{x},yz,yz} = t_2 = 1.25 \\ t_{i,i\pm\hat{x}\pm\hat{y},xz,xz} &= t_{i,i\pm\hat{x}\pm\hat{y},yz,yz} = t_3 = -0.9 \\ t_{i,i+\hat{x}-\hat{y},xz,yz} &= t_{i,i+\hat{x}-\hat{y},yz,xz} = t_{i,i-\hat{x}+\hat{y},xz,yz} \\ &= t_{i,i+\hat{x}-\hat{y},yz,xz} = t_4 = -0.85 \\ t_{i,i+\hat{x}+\hat{y},xz,yz} &= t_{i,i+\hat{x}+\hat{y},yz,xz} = t_{i,i-\hat{x}-\hat{y},xz,yz} \\ &= t_{i,i-\hat{x}-\hat{y},yz,xz} = -t_4. \end{aligned} \quad (3)$$

Here, \hat{x} and \hat{y} denote the unit vector along the x and y direction, respectively.

The second term accounts for the superconducting pairing. Considering that a main purpose here is to address the effects of the magnetic vortices and nonmagnetic impurities on the spin-lattice relaxation rate in the iron-based superconductors, we take a phenomenological form for the intra-orbital pairing interaction,

$$H_{pair} = \sum_{ij,\alpha} V_{ij} (\Delta_{ij,\alpha\alpha} c_{i,\alpha\uparrow}^\dagger c_{j,\alpha\downarrow}^\dagger + h.c.) \quad (4)$$

with V_{ij} as the strengths of effective attractions.

Thus, we obtain the Bogoliubov-de Gennes equations for this model Hamiltonian³³

$$\sum_{j,\alpha < \beta} \begin{pmatrix} H_{ij,\alpha\alpha,\sigma} & \Delta_{ij,\alpha\alpha} & H_{ij,\alpha\beta,\sigma} & 0 \\ \Delta_{ij,\alpha\alpha}^* & -H_{ij,\alpha\alpha,\bar{\sigma}}^* & 0 & -H_{ij,\alpha\beta,\bar{\sigma}}^* \\ H_{ij,\alpha\beta,\sigma} & 0 & H_{ij,\beta\beta,\sigma} & \Delta_{ij,\beta\beta} \\ 0 & -H_{ij,\alpha\beta,\bar{\sigma}}^* & \Delta_{ij,\beta\beta}^* & -H_{ij,\beta\beta,\bar{\sigma}}^* \end{pmatrix} \times \begin{pmatrix} u_{j,\alpha,\sigma}^n \\ v_{j,\alpha,\bar{\sigma}}^n \\ u_{j,\beta,\sigma}^n \\ v_{j,\beta,\bar{\sigma}}^n \end{pmatrix} = E_n \begin{pmatrix} u_{i,\alpha,\sigma}^n \\ v_{i,\alpha,\bar{\sigma}}^n \\ u_{i,\beta,\sigma}^n \\ v_{i,\beta,\bar{\sigma}}^n \end{pmatrix}, \quad (5)$$

where,

$$\begin{aligned} H_{ij,\alpha\alpha,\sigma} &= -e^{i\varphi_{ij}} t_{ij,\alpha\alpha} - \mu \\ H_{ij,\alpha\beta(\beta \neq \alpha),\sigma} &= -e^{i\varphi_{ij}} t_{ij,\alpha\beta(\beta \neq \alpha)}. \end{aligned} \quad (6)$$

$u_{j,\alpha,\sigma}^n$ ($u_{j,\beta,\bar{\sigma}}^n$), $v_{j,\alpha,\sigma}^n$ ($v_{j,\beta,\bar{\sigma}}^n$) are the Bogoliubov quasiparticle amplitudes on the j -th site with corresponding eigenvalues E_n .

The pairing amplitude and electron densities are obtained through the following self-consistent equations,

$$\begin{aligned} \Delta_{ij,\alpha\alpha} &= \frac{V_{ij}}{4} \sum_n (u_{i,\alpha,\sigma}^n v_{j,\alpha,\bar{\sigma}}^{n*} + v_{i,\alpha,\bar{\sigma}}^{n*} u_{j,\alpha,\sigma}^n) \times \\ &\quad \tanh\left(\frac{E_n}{2k_B T}\right) \\ n_{i,\alpha,\uparrow} &= \sum_n |u_{i,\alpha,\uparrow}^n|^2 f(E_n) \\ n_{i,\alpha,\downarrow} &= \sum_n |v_{i,\alpha,\downarrow}^n|^2 [1 - f(E_n)]. \end{aligned} \quad (7)$$

The site-averaged DOS $N(E)$ is calculated by

$$\begin{aligned} N(E) &= -\frac{1}{N} \sum_i \sum_{n,\alpha} [|u_{i,\alpha,\uparrow}^n|^2 f'(E_n - E) \\ &\quad + |v_{i,\alpha,\downarrow}^n|^2 f'(E_n + E)], \end{aligned} \quad (8)$$

where, $f'(E)$ is the derivative of the Fermi-Dirac distribution function with respect to energy. The nuclear spin-lattice relaxation rate is given by³⁴

$$\begin{aligned} R(r_i, r_{i'}) &= \text{Im}\chi_{+,-}(r_i, r_{i'}, i\Omega_n \rightarrow \Omega + i\eta)/(\Omega/T)|_{\Omega \rightarrow 0} \\ &= -\sum_{n, n'} [\mathcal{U}_i^n \mathcal{U}_{i'}^{n*} \mathcal{V}_i^{n'} \mathcal{V}_{i'}^{n'*} - \mathcal{V}_i^n \mathcal{U}_i^{n*} \mathcal{U}_{i'}^{n'} \mathcal{V}_{i'}^{n'*}] \\ &\quad \times \pi T f'(E_n) \delta(E_n - E_{n'}). \end{aligned} \quad (9)$$

Here, $\mathcal{U}_i^n = u_{i,\alpha}^n + u_{i,\beta}^n$ and $\mathcal{V}_i^n = v_{i,\alpha}^n + v_{i,\beta}^n$. We choose $\mathbf{r}_i = \mathbf{r}_{i'}$ because the nuclear spin-lattice relaxation at a local site is dominant. Then the site-dependent relaxation time is given by $T_1(r) = 1/R(r, r)$ and the bulk relaxation time $T_1 = (1/N) \sum_r T_1(r)$.

In numerical calculations, V_{ij} is chosen to give a short coherence length of a few lattice spacing in the SC state being consistent with experiments.³⁵ Under the conditions $V_{ij} \sim 2.0$, $\mu = 1.2$ at temperature $T = 1 \times 10^{-5}$, the filling factor $n = \sum_{i,\alpha,\sigma} (n_{\alpha,\sigma}) / (N_x N_y) = 1.9$ and the coherent peak of the SC order parameter in the DOS is at $\Delta_{max} \sim 0.25$. Thus, we estimate the coherence length $\xi_0 \sim E_F a / |\Delta_{max}| \sim 5a$,³⁶ with a being the Fe-Fe distance on the square lattice. Due to this short coherence length, presumably the system will be a type-II superconductor. To study the vortex states, we employ the magnetic unit cell with size $N_x \times N_y = 48 \times 24$ that accommodates two magnetic vortices, unless otherwise specified. In view of these parameters, we estimate the upper critical field $B_{c2} \sim 100T$. Therefore, the model calculation is particularly suitable for the iron-based type-II superconductors such as $\text{CaFe}_{1-x}\text{Co}_x\text{AsF}$, $\text{Eu}_{0.7}\text{Na}_{0.3}\text{Fe}_2\text{As}_2$ and $\text{FeTe}_{1-x}\text{S}_x$, where the typical coherence length ξ_0 deduced from the experiments is of a few lattice spacing and the upper critical field achieves as high as dozens of Tesla.³⁵

III. RESULTS AND DISCUSSION

Since no final consensus on the SC pairing symmetry has yet been achieved, we choose three possible singlet pairing symmetries, i.e., the most popular sign-reversed s_{\pm} -wave, the on-site s -wave and the d -wave symmetries with their respective gap functions $\Delta_{s_{\pm}} = \Delta_0 \cos(k_x) \cos(k_y)$, $\Delta_s = \Delta_0$ and $\Delta_d = \Delta_0 [\cos(k_x) - \cos(k_y)]$ to carry out the contrasting study. At the end of this section, we will also touch on another possibility of the s_{\pm} -wave with angular variation along the electron Fermi pockets, which will be referred to as s_h -wave. In order to obtain comparable values of critical temperature T_c in the self-consistent calculations, we set respectively $V_{ij} = 1.6$ for s_{\pm} -wave, $V_{ij} = 2.0$ for s -wave, and $V_{ij} = 1.8$ for d -wave pairing symmetries.

To begin with, we briefly summarize the site-averaged DOS spectra $N(E)$ in the uniform SC state at $T = 1 \times 10^{-5}$ as shown by the solid lines in Fig. 1. For the s_{\pm} - and s -wave symmetries, no node exists in the gap along the Fermi surfaces. Correspondingly, the full gap

structures can be seen in the DOS as shown in Figs. 1(a) and 1(b). In the d -wave symmetry, the gap function has line nodes at $k_x = k_y$, which cross the hole pocket but do not intersect the electron pocket. As a result, the DOS consists of a small V-shaped gap structure at very low energy and a U-shaped gap structure at higher energy as shown in Fig. 1(c), which exhibits a difference from that in high- T_c cuprates.

Next, we show the DOS in the magnetic vortex state and in the presence of nonmagnetic impurities as presented by the dotted and dashed lines in Fig. 1, respectively. In the vortex state, the application of a magnetic field will induce the quasiparticle flow around the vortex core, such that the nodal line will appear in the otherwise fully gaped SC state due to an additional Doppler shift in the quasiparticle energy, giving rise to the V-shaped gap structures for the s_{\pm} - and s -wave symmetries, as shown in Figs. 1(a) and 1(b). In contrast, in the presence of impurities, the DOS shows the V-shaped structure for the s_{\pm} -wave symmetry but the U-shaped for the s -wave symmetry [Figs. 1(a) and 1(b)]. This is due to the fact that the impurity potential has intra- and inter-band components for the multiband materials. The intra-band components scatter fermions that have the same sign for the s_{\pm} -wave SC order parameter and therefore do not affect the superconductivity. Whereas the inter-band components scatter fermions with opposite SC order parameters, thus have the pairing breaking effect. As a result, they yield an obvious decrease in T_c and simultaneously introduce the V-shaped feature in DOS. In the case of the s -wave symmetry, no sign change in the SC order parameters occurs on both the electron and hole pockets, so that no obvious pairing breaking effect is induced by the impurities and the U-shaped DOS is untouched.

For the d -wave symmetry, the small V-shaped superconducting gap is filled by the low energy quasiparticles induced by either vortices or impurities, resulting in a pseudogap-like U-shaped feature with finite density at Fermi energy, as indicated by the dotted and dashed lines in Fig. 1(c). The line nodes existing on the hole-pocket in the d -wave symmetry make it vulnerable to the impurities, resulting in the disappearance of the small V-shaped structure. However, the full gap opening on the electron-pocket is robust against impurities, so that the pseudogap-like U-shaped feature is obtained. In the vortex state, since the quasiparticles induced by the vortex come preferably from the line nodes, the pseudogap-like U-shaped structure remains. The results in Fig. 1 indicate that the characteristic low energy quasiparticle excitations depend on the gap functions in the presence of magnetic vortices and nonmagnetic impurities.

Now, we turn to the discussion of the temperature (T) dependence of the nuclear relaxation rate. For the uniform SC state, both the s_{\pm} - and s -wave symmetries produce a power law relation $T_1^{-1} \sim T^5$ below T_c and it evolves into an exponential dependence at very low temperature, as shown by the solid lines in Figs. 2 and 3,³⁷ which are the consequence of the full-gap DOS in Fig. 1.

In the vortex state, due to the similar V-shaped DOS for both the s_{\pm} - and s -wave symmetries, T_1^{-1} changes its T dependence to T^3 below T_c and becomes nearly proportional to T for the s_{\pm} -wave symmetry while $T^{1.5}$ for the s -wave symmetry at low temperature, as denoted by the dotted lines in Figs. 2(a) and 3(a), respectively. [The dotted lines in Figs. 2(a)-5(a) show the results for magnetic unit cell with size 48×24 , while the dash-dotted lines in these figures the results for magnetic unit cell with size 40×20 .]

We note that both the T^3 dependence and the low- T feature with nearly linear slop are reminiscent of the experimental observations,^{13,14} where the T -linear dependence has been regarded as the evidence for a residual density of states at zero energy in SC state. As mentioned above, although the s_{\pm} -wave pairing is basically the full gap, the application of a magnetic field will cause the quasiparticle flow around the vortex core, such that the nodal line will appear in the SC state due to an additional Doppler shift quasiparticle energy, giving rise to the V-shaped DOS and T^3 dependent relaxation rate. In view of this, we may expect that the slop of temperature dependent T_1^{-1} should be insensitive to the strength of the magnetic field, which has already been observed in experiment.²⁹ This is evident by the comparison between the dotted- and dash-dotted-curves shown in Fig. 2(a), where the magnetic field for the dash-dotted-curve is about 1.5 times as large as that for the dotted-curve.

A striking difference between the s_{\pm} -wave and the s -wave states in the T -dependence of T_1^{-1} appears when the effect of the impurity scattering is considered, as shown in Figs. 2(b) and 3(b). For the s_{\pm} -wave state, T_1^{-1} deviates gradually from T^5 to an overall T^3 behavior at weak disorder such as $U = 1$, then to a T linear dependence at low temperatures as the disorder strength U is increased to about $U = 1.5$, which depicts the sensitivity of the SC order to the impurities and is in accordance with the DOS results. On the other hand, T_1^{-1} changes little upon the introduction of the disorder for the s -wave symmetry. We also notice that T_c is reduced substantially for the s_{\pm} -wave symmetry at the moderate and even the weak disorder strength, as can be seen from the lower- T shift of the inflexion point on the curves in Fig. 2(b). This again reflects the fact that the sign-reversed s_{\pm} -wave pairing is fragile against the nonmagnetic impurities, which has also been predicted theoretically by adopting a more sophisticated orbital model and conformed experimentally in the specific heat and resistivity measurements.^{27,38,39}

In Fig. 4, we present the results for the d -wave symmetry. Unlike the formers, the overall T -dependence of T_1^{-1} in the uniform SC state roughly follows T^3 relation due to the existing of nodal line in the gap structure. When a magnetic field is applied, T_1^{-1} exhibits a T -linear dependence at low temperatures, though a T^3 behavior following T_c still remains. We notice that this trend is rather robust against the magnitude of the magnetic field, as the results for two cases are nearly the same though their magnitude differs about 1.5 times, as shown

in Fig. 4(a). Thus, for the three different pairing states, T_1^{-1} exhibits nearly similar T -dependence in the magnetic vortex state, due to the presence of quasiparticles induced by the vortex. In the presence of impurities, T_1^{-1} for both the d -wave and the s_{\pm} -wave symmetries exhibit a consecutive change from the T^3 to T -linear dependence when temperature is decreased, which contrasts with that for the s -wave state.

We notice that the actual multiple Fermi surface sheets in iron-based superconductors are not exactly reproduced by the two-orbital model, so the general structure of the gap in the s_{\pm} -wave channel may involve the angular variation along the electron Fermi pockets and have the form $\Delta_h = \Delta_0\{\cos(k_x)\cos(k_y) + h[\cos(k_x) + \cos(k_y)]\}$, where the factor h measures the strength of the angular dependent variations along the electron Fermi pockets.⁴⁰⁻⁴⁴ In the case of $h > 1$, there will be accidental nodes along the electron Fermi pockets,⁴⁵ which will be focused here. Such accidental nodes are reflected in the V-shaped DOS in Fig. 1(d) and nearly T^4 dependence of T_1^{-1} for the typical results with $h = 1.5$ in the uniform SC state [Fig. 5]. This result differs from the T^3 dependence for the symmetry imposed nodal behavior such as in the case of the d -wave state. Although the T -dependence of T_1^{-1} in the vortex state is much like that of the s_{\pm} -wave case, it is less influenced by the impurities [see Fig. 5].

IV. CONCLUSION

In conclusion, we have investigated the effect of the magnetic field and nonmagnetic impurities on the DOS and the spin-lattice relaxation rate T_1^{-1} in the iron-based superconductors. It is shown that the characteristic site-averaged DOS depends on the gap functions in the presence of magnetic vortices and nonmagnetic impurities. The magnetic vortices have a significant contribution to the spin-lattice relaxation rate and lead to the relation $T_1^{-1} \sim T^3$ followed by a nearly T -linear dependence at low temperatures for all three symmetries (s_{\pm} -, s - and d -wave) considered here, though in the clean uniform state a T^3 dependence for the d -wave symmetry differentiates from the others with a T^5 dependence. In the presence of nonmagnetic impurities, this enhancement of T_1^{-1} can only be seen for the s_{\pm} - and d -wave symmetries, whereas it is almost unaffected for the s -wave symmetry. Our results suggest that it is impossible to distinguish the s_{\pm} - and d -wave symmetries on the basis of the measurements of spin-lattice relaxation rates when a magnetic field and/or impurity scatterings are present.

V. ACKNOWLEDGEMENT

This work was supported by the National Natural Science Foundation of China (Grant No. 10904062 and No. 91021001), Hangzhou Normal University (HSKQ0043, HNUEYT), and the Ministry of Science and Technol-

ogy of China (973 project Grants Nos. 2011CB922101, 2011CB605902).

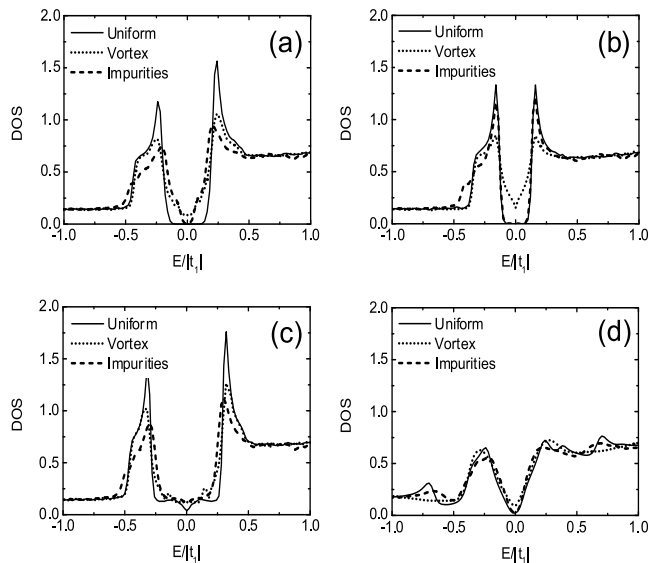


FIG. 1: Site-averaged DOS for the s_{\pm} -wave in (a), the s -wave in (b), the d -wave in (c), and the s_h -wave in (d) (see text). The DOS in the uniform SC state is plotted with solid lines. The results in the magnetic vortex state and those in the presence of nonmagnetic impurities are shown with the dotted and dashed lines, respectively.

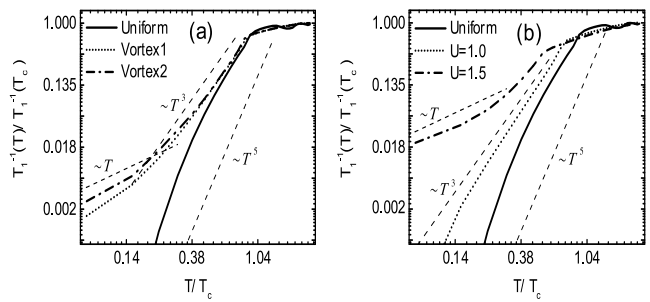


FIG. 2: T -dependence of T_1^{-1} shown in the double logarithmic chart for s_{\pm} -wave symmetry in the vortex state (a), and in the presence of nonmagnetic impurities (b). The dotted and dash-dotted curves denote different strength of the magnetic field (see text) and the impurity scattering. The results for the uniform SC state are also plotted with solid line in each figure.

- ¹ Y. Kamihara, T. Watanabe, M. Hirano, and H. Hosono, *J. Am. Chem. Soc.* **130**, 3269 (2008).
- ² X. H. Chen, T. Wu, G. Wu, R. H. Liu, H. Chen, and D. F. Fang, *Nature* **453**, 761 (2008).
- ³ Z.-A. Ren, G.-C. Che, X.-L. Dong, J. Yang, W. Lu, W. Yi, X.-L. Shen, Z.-C. Li, L.-L. Sun, F. Zhou, and Z.-X. Zhao, *Europhys. Lett.* **83**, 17002 (2008).
- ⁴ G. F. Chen, Z. Li, D. Wu, G. Li, W. Z. Hu, J. Dong, P. Zheng, J. L. Luo, and N. L. Wang, *Phys. Rev. Lett.* **100**, 247002 (2008).
- ⁵ C. Wang, L. Li, S. Chi, Z. Zhu, Z. Ren, Y. Li, Y. Wang, X. Lin, Y. Luo, S. Jiang, X. Xu, G. Cao, and Z. Xu, *Europhys. Lett.* **83**, 67006 (2008).
- ⁶ C. de la Cruz, Q. Huang, J. W. Lynn, J. Li, W. Ratcliff II, J. L. Zarestky, H. A. Mook, G. F. Chen, J. L. Luo, N. L. Wang, and P. Dai, *Nature* **453**, 899 (2008).
- ⁷ J. Dong, H. J. Zhang, G. Xu, Z. Li, G. Li, W. Z. Hu, D. Wu, G. F. Chen, X. Dai, J. L. Luo, Z. Fang, and N. L. Wang, *Europhys. Lett.* **83**, 27006 (2008).
- ⁸ I. I. Mazin, D. J. Singh, M. D. Johannes, and M. H. Du, *Phys. Rev. Lett.* **101**, 057003 (2008); A. V. Chubukov, D. V. Efremov, and I. Eremin, *Phys. Rev. B* **78**, 134512 (2008).
- ⁹ K. Kuroki, S. Onari, R. Arita, H. Usui, Y. Tanaka, H. Kontani, and H. Aoki, *Phys. Rev. Lett.* **101**, 087004 (2008); V. Cvetkovic, and Z. Tesanovic, *Phys. Rev. B* **80**, 024512 (2009).
- ¹⁰ Z. J. Yao, J. X. Li, and Z. D. Wang, *New J. Phys.* **11**, 025009 (2009); S. L. Yu, J. Kang, and J. X. Li, *Phys. Rev.*

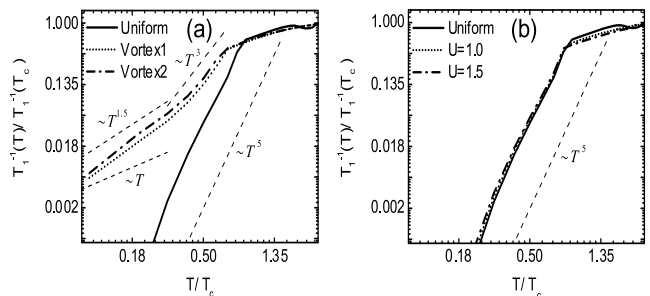


FIG. 3: T -dependence of T_1^{-1} shown in the double logarithmic chart for s -wave symmetry in the vortex state (a), and in the presence of nonmagnetic impurities (b). The dotted and dash-dotted curves denote different strength of the magnetic field (see text) and the impurity scattering. The results for the uniform SC state are also plotted with solid line in each figure.

B **79**, 064517 (2009).

- ¹¹ W.-Q. Chen, K.-Y. Yang, Y. Zhou, and F.-C. Zhang, *Phys. Rev. Lett.* **102**, 047006 (2009); F. Wang, H. Zhai, Y. Ran, A. Vishwanath, and D. H. Lee, *Phys. Rev. Lett.* **102**, 047005 (2009).
- ¹² H.-J. Grafe, D. Paar, G. Lang, N. J. Curro, G. Behr, J. Werner, J. Hamann-Borrero, C. Hess, N. Leps, R. Klingeler, and B. Büchner, *Phys. Rev. Lett.* **101**, 047003

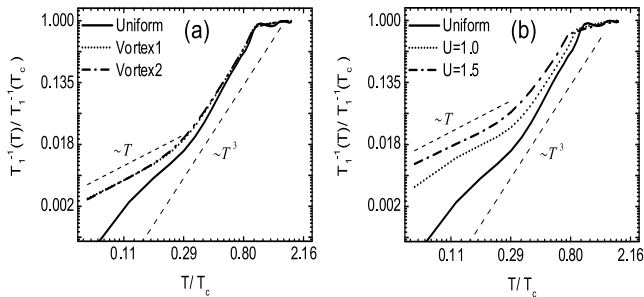


FIG. 4: T -dependence of T_1^{-1} shown in the double logarithmic chart for d -wave symmetry in the vortex state (a), and in the presence of nonmagnetic impurities (b). The dotted and dash-dotted curves denote different strength of the magnetic field (see text) and the impurity scattering. The results for the uniform SC state are also plotted with solid line in each figure.

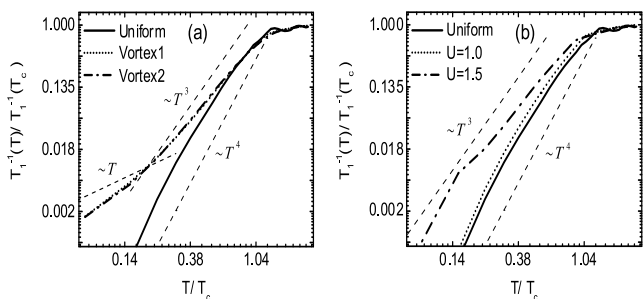


FIG. 5: T -dependence of T_1^{-1} shown in the double logarithmic chart for s_h -wave symmetry (see text) in the vortex state (a), and in the presence of nonmagnetic impurities (b). The dotted and dash-dotted curves denote different strength of the magnetic field (see text) and the impurity scattering. The results for the uniform SC state are also plotted with solid line in each figure.

(2008).

13 Y. Nakai, T. Iye, S. Kitagawa, K. Ishida, S. Kasahara, T. Shibauchi, Y. Matsuda, and T. Terashima, Phys. Rev. B **81**, 020503(R) (2010).

14 F. Hammerath, S.-L. Drechsler, H.-J. Grafe, G. Lang, G. Fuchs, G. Behr, I. Eremin, M. M. Korshunov, and B. Büchner, Phys. Rev. B **81**, 140504 (2010).

15 H.-S. Lee, M. Bartkowiak, J.-H. Park, J.-Y. Lee, J.-Y. Kim, N.-H. Sung, B. K. Cho, C.-U. Jung, J. S. Kim, and H.-J. Lee, Phys. Rev. B **80**, 144512 (2009).

16 K. Matano, Z. A. Ren, X. L. Dong, L. L. Sun, Z. X. Zhao, and G. Q. Zheng, Europhys. Lett. **83**, 57001 (2008).

17 S. Kawasaki, K. Shimada, G. F. Chen, J. L. Luo, N. L. Wang, and G. Q. Zheng, Phys. Rev. B **78**, 220506 (R) (2008).

18 K. Matano, G. L. Sun, D. L. Sun, C. T. Lin, and G. Q. Zheng, Europhys. Lett. **87**, 27012 (2009).

19 S. W. Zhang, L. Ma, Y. D. Hou, J. Zhang, T.-L. Xia, G. F. Chen, J. P. Hu, G. M. Luke, and W. Yu, Phys. Rev. B **81**, 012503 (2010).

20 M. Yashima, H. Nishimura, H. Mukuda, Y. Kitaoka, K. Miyazawa, P. M. Shirage, K. Kihou, H. Kito, H. Eisaki,

and A. Iyo, J. Phys. Soc. Jpn. **78**, 103702 (2009).

21 H. Fukazawa, T. Yamazaki, K. Kondo, Y. Kohori, N. Takeshita, P. M. Shirage, K. Kihou, K. Miyazawa, H. Kito, H. Eisaki, and A. Iyo, J. Phys. Soc. Jpn. **78**, 033704 (2009).

22 H. Fukazawa, Y. Yamada, K. Kondo, T. Saito, Y. Kohori, K. Kuga, Y. Matsumoto, S. Nakatsuji, H. Kito, P. M. Shirage, K. Kihou, N. Takeshita, C. H. Lee, A. Iyo, and H. Eisaki, J. Phys. Soc. Jpn. **78**, 083712 (2009).

23 C. Michioka, H. Ohta, M. Matsui, J. Yang, K. Yoshimura, and M. Fang, arXiv:0911.3729 (unpublished).

24 D. Parker, O. V. Dolgov, M. M. Korshunov, A. A. Golubov, and I. I. Mazin, Phys. Rev. B **78**, 134524 (2008).

25 Y. Senga, and H. Kontani, New J. Phys. **11**, 035005 (2009).

26 Y. Bang, Han-Yong Choi, and H. Won, Phys. Rev. B **79**, 054529 (2009).

27 S. Onari, and H. Kontani, Phys. Rev. Lett. **103**, 177001 (2009).

28 S. Onari, and H. Kontani, Phys. Rev. Lett. **106**, 259702 (2011).

29 L. Ma, J. Zhang, G. F. Chen, T.-L. Xia, J. B. He, D. M. Wang, and W. Yu, arXiv:1003.2775 (unpublished).

30 K. Kitagawa, N. Katayama, H. Gotou, T. Yagi, K. Ohgushi, T. Matsumoto, Y. Uwatoko, and M. Takigawa, Phys. Rev. Lett. **103**, 257002 (2009).

31 S. Raghu, X.-L. Qi, C.-X. Liu, D. J. Scalapino, and S.-C. Zhang, Phys. Rev. B **77**, 220503(R) (2008).

32 G. Xu, W. Ming, Y. Yao, X. Dai, S.-C. Zhang and Z. Fang, Europhys. Lett. **82**, 67002 (2008); Z. P. Yin, S. Lebègue, M. J. Han, B. P. Neal, S. Y. Savrasov, and W. E. Pickett, Phys. Rev. Lett. **101**, 047001 (2008).

33 H.-M. Jiang, J.-X. Li, and Z. D. Wang, Phys. Rev. B **80**, 134505 (2009).

34 M. Takigawa, M. Ichioka, and K. Machida, Phys. Rev. Lett. **83**, 3057 (1999); *ibid.* **90**, 047001 (2003); M. Takigawa, M. Ichioka, K. Kuroki, Y. Asano, and Y. Tanaka, *ibid.* **97**, 187002 (2006).

35 S. Takeshita, R. Kadono, M. Hiraishi, M. Miyazaki, A. Koda, S. Matsuishi, and H. Hosono, Phys. Rev. Lett. **103**, 027002 (2009); Y. Qi, Z. Gao, L. Wang, D. Wang, X. Zhang, and Y. Ma, New J. Phys. **10**, 123003 (2008); Y. Mizuguchi, F. Tomioka, S. Tsuda, T. Yamaguchi, and Y. Takano, Appl. Phys. Lett. **94**, 012503 (2009).

36 Y. D. Zhu, F. C. Zhang, and M. Sigrist, Phys. Rev. B **51**, 1105 (1995).

37 A. B. Vorontsov, and I. Vekhter, Phys. Rev. Lett. **105**, 187004 (2010).

38 G. Mu, B. Zeng, P. Cheng, Z. Wang, L. Fang, B. Shen, L. Shan, C. Ren, H.-H. Wen, Chin. Phys. Lett. **27**, 037402 (2010).

39 Y. F. Guo, Y. G. Shi, S. Yu, A. A. Belik, Y. Matsushita, M. Tanaka, Y. Katsuya, K. Kobayashi, I. Nowik, I. Felner, V. P. S. Awana, K. Yamaura, and E. Takayama-Muromachi, Phys. Rev. B **82**, 054506 (2010); J. J. Li, Y. F. Guo, S. B. Zhang, S. Yu, Y. Tsujimoto, K. Yamaura, E. Takayama-Muromachi, Physica C **471**, 213 (2011).

40 A. V. Chubukov, M. G. Vavilov, and A. B. Vorontsov, Phys. Rev. B **80**, 140515(R) (2009).

41 D. N. Basov, and A. V. Chubukov, Nature Phys. **7**, 272 (2011).

42 S. Maiti, and A. V. Chubukov, Phys. Rev. B **82**, 214515 (2010).

43 A. F. Kemper, T. A. Maier, S. Graser, H.-P. Cheng, P. J. Hirschfeld, and D. J. Scalapino, New J. Phys. **12**, 073030 (2010).

- ⁴⁴ S. Maiti, M. M. Korshunov, T. A. Maier, P. J. Hirschfeld, A. V. Chubukov, arXiv:1104.1814 (unpublished).
- ⁴⁵ S. Maiti, A. V. Chubukov, arXiv:1104.2923 (unpublished).